Article

Cell Reports

Histone Deacetylases Positively Regulate Transcription through the Elongation Machinery

Graphical Abstract

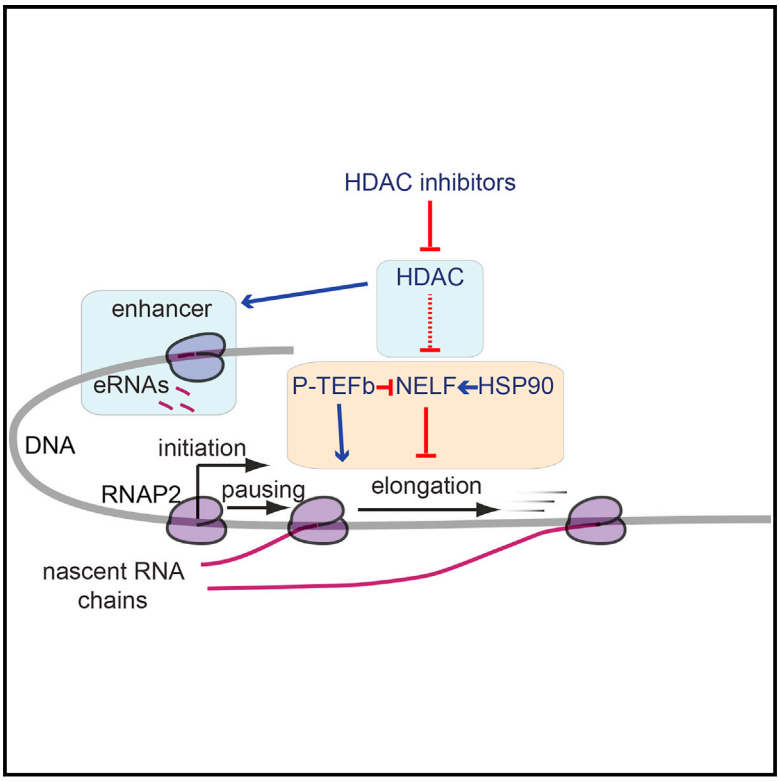

Authors

Celeste B. Greer, Yoshiaki Tanaka, Yoon Jung Kim, Peng Xie, Michael Q. Zhang, In-Hyun Park, Tae Hoon Kim

Correspondence

genome@utdallas.edu

In Brief

Greer et al. use a combination of GRO-seq, ChIP-seq, and small molecule inhibitors to probe the mechanisms of transcription elongation across the human genome. They determine that histone deacetylases stimulate transcription elongation by mechanisms involving eRNA production at enhancers and eviction of NELF at promoters.

Highlights

- HDAC inhibitor-mediated elongation repression requires HSP90
- BRD4 binding to promoters and enhancers is reduced upon HDAC inhibition
- HDAC inhibition results in loss of enhancer RNA synthesis

Greer et al., 2015, Cell Reports *13*, 1444–1455
November 17, 2015
http://dx.doi.org/10.1016/j.celrep.2015.10.013

CellPress

OPEN ACCESS
CellPress

Cell Reports
Article

Histone Deacetylases Positively Regulate Transcription through the Elongation Machinery

Celeste B. Greer,[1] Yoshiaki Tanaka,[2] Yoon Jung Kim,[3] Peng Xie,[3] Michael Q. Zhang,[3] In-Hyun Park,[2] and Tae Hoon Kim[3,*]
[1]Department of Pharmacology, Yale University School of Medicine, New Haven, CT 06520, USA
[2]Department of Genetics and Stem Cell Center, Yale University School of Medicine, New Haven, CT 06520, USA
[3]Department of Biological Sciences and Center for Systems Biology, The University of Texas at Dallas, Richardson, TX 75080, USA
*Correspondence: genome@utdallas.edu
http://dx.doi.org/10.1016/j.celrep.2015.10.013

SUMMARY

Transcription elongation regulates the expression of many genes, including oncogenes. Histone deacetylase (HDAC) inhibitors (HDACIs) block elongation, suggesting that HDACs are involved in gene activation. To understand this, we analyzed nascent transcription and elongation factor binding genome-wide after perturbation of elongation with small molecule inhibitors. We found that HDACI-mediated repression requires heat shock protein 90 (HSP90) activity. HDACIs promote the association of RNA polymerase II (RNAP2) and negative elongation factor (NELF), a complex stabilized by HSP90, at the same genomic sites. Additionally, HDACIs redistribute bromodomain-containing protein 4 (BRD4), a key elongation factor involved in enhancer activity. BRD4 binds to newly acetylated sites, and its occupancy at promoters and enhancers is reduced. Furthermore, HDACIs reduce enhancer activity, as measured by enhancer RNA production. Therefore, HDACs are required for limiting acetylation in gene bodies and intergenic regions. This facilitates the binding of elongation factors to properly acetylated promoters and enhancers for efficient elongation.

INTRODUCTION

Transcription elongation is a critical step in regulating many human genes (Adelman and Lis, 2012; Gilchrist et al., 2010). We have reported previously that inhibition of histone deacetylase (HDAC) activity results in a dramatic decrease in transcription elongation efficiency at multiple genes using global run-on sequencing (GRO-seq) (Core et al., 2008) to analyze RNA polymerase II (RNAP2) activity across the genome. We found that elongation repression occurs in several cell lines derived from both non-cancerous tissue and tumors, suggesting that this is a general effect of inhibiting HDACs in human cells (Kim et al., 2013). As a pivotal determinant of transcript level for many oncogenes, elongation is being investigated for cancer therapy because it is regulated by many factors targetable by small molecule inhibitors (Delmore et al., 2011; Zhai et al., 2002; Zuber et al., 2011). HDAC inhibitors (HDACIs) are used clinically in tumor treatment and inhibit the zinc-dependent HDAC isoforms, which are often components of complexes associated with transcriptional silencing.

Transcription of protein-coding genes by RNAP2 can be regulated at initiation and elongation steps (Adelman and Lis, 2012). Initiation of transcription is catalyzed by the assembly of the pre-initiation complex at the promoter (Thomas and Chiang, 2006), followed by the incorporation of the first several nucleotides downstream from the promoter (Core et al., 2008). Transcription through the gene body by the RNAP2 is prevented by factors that block elongation, such as negative elongation factor (NELF) and dichloro-1-β-D-ribofuranosylbenzimidazole (DRB)-sensitivity inducing factor (DSIF) (Kwak and Lis, 2013). For RNAP2 to transition into the productive elongation phase and synthesize full-length pre-mRNA, elongation-inducing factors are recruited. Positive transcription elongation factor b (P-TEFb), which modifies RNAP2 and other factors required for overcoming the elongation block, is recruited by BRD4, an acetyl-lysine binding protein (Jang et al., 2005; Yang et al., 2005). P-TEFb contains cyclin-dependent kinase 9 (CDK9), which phosphorylates DSIF, NELF, and serine 2 of the heptad repeats in the C-terminal domain (CTD) of the largest subunit of RNAP2 (Fujinaga et al., 2004). NELF can interact with nascent RNAs and is evicted when elongation is induced (Yamaguchi et al., 1999), whereas DSIF travels along with the elongating RNAP2 upon phosphorylation by P-TEFb (Wu et al., 2003).

It was surprising that HDACIs are capable of directly repressing the transcription of many genes (Chou et al., 2011; Kim et al., 2013; Scott et al., 2002), given that classical HDACs are components of complexes known to silence transcription. The two inhibitors used here, trichostatin A (TSA) and suberanilohydroxamic acid (SAHA, known clinically as vorinostat), inhibit the 11 classical HDAC isoforms (Bolden et al., 2006). They are found in the Sin3, nucleosome-remodeling deacetylase (NuRD), and nuclear receptor corepressor 2/silencing mediator for retinoid or thyroid hormone receptors (NCOR2/SMRT) complexes (Glass and Rosenfeld, 2000). Lysine acetylation is a well-known mark of transcriptionally active open chromatin (Eberharter and Becker, 2002), and acetylation of many transcription factors activates their function, and deacetylation

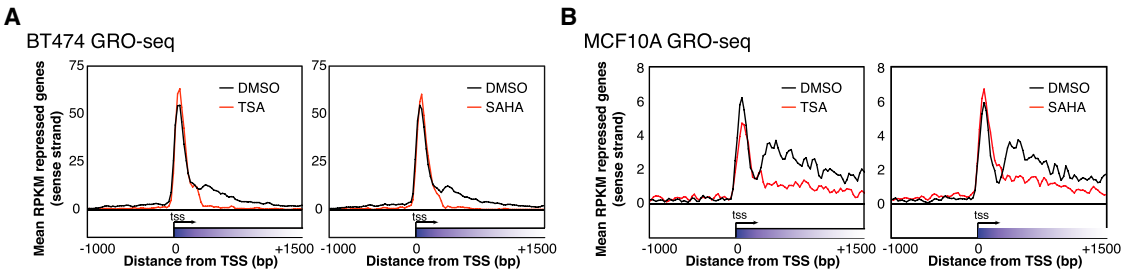

Figure 1. HDACIs Block Elongation of RNAP2 Transcription in the Genes They Repress

(A) Metagene plots of GRO-seq RPKM in the sense direction for repressed genes in BT474 cells. Repressed genes had significantly (log-likelihood ratio $p < 10^{-20}$, one GRO-seq experiment) reduced RPKM in the gene body (300 bp downstream of TSSs to gene ends). 6,354 repressed genes were analyzed for TSA and 7,389 for SAHA.

(B) Same as (A) for MCF10A cells. There were 3,866 repressed genes for TSA and 4,643 for SAHA.

See Figure S1 for GRO-seq statistics, RNAP2 ChIP-seq, GRO-seq of a shorter treatment of SAHA in BT474 cells, SAHA blocking elongation in another cell line, and validation that SAHA and TSA repress transcription through their effects on HDACs. See Table S1 for the number of genes common to each expression change subgrouping between the GRO-seq shown here and previously published GRO-seq data. See Table S2 for median fold changes in subclassifications of gene expression changes for different factors by ChIP-seq in promoter regions. See Table S3 for median fold changes in subclassifications of gene expression changes for different factors by ChIP-seq in gene body regions.

represses their function (Sterner and Berger, 2000). However, in support of a role for HDACs in active transcription, prior research has shown that HDAC complexes are involved in both repression and activation of transcription in yeast (Vidal and Gaber, 1991; Vidal et al., 1991; Wang et al., 2002), and some transcription factors are activated when deacetylated (Chen et al., 1999; Wolf et al., 2002; Xu et al., 2003). These proteins appear to facilitate similar opposing functions in higher eukaryotes as well because HDACs are associated strongly with actively transcribed genes in human cells (Wang et al., 2009).

Enhancers are transcriptional regulatory elements that promote the transcription of a gene or genes (Moreau et al., 1981; Shlyueva et al., 2014). From a linear perspective of DNA sequences, they are often located far away from the transcription start sites (TSSs) of genes, but folding and looping of the chromosome can bring these elements into close proximity of the genes whose transcription they affect (Jin et al., 2013). Recently, active enhancers have been found to be sites of bidirectional transcription and create unstable transcripts called enhancer RNA (eRNA). eRNAs are reliable markers of active enhancers (Danko et al., 2015), and the amount of eRNA produced relates to the activity of the enhancer. Knockdown of eRNAs reduces the transcription of the target genes of an enhancer (Banerjee et al., 2014; Hsieh et al., 2014; Melo et al., 2013). BRD4 is strongly associated with enhancers, and repression of BRD4 results in a block of elongation in target genes of enhancers (Lovén et al., 2013). NELF may be involved in the link between enhancers and the promoters they induce as well because it has an RNA-interacting domain that binds paused transcripts and, potentially, eRNAs as well (Yamaguchi et al., 1999, 2002). It has been postulated that the NELF-induced elongation block is overcome when the RNA-interacting domain exchanges the paused transcript for an eRNA (Schaukowitch et al., 2014).

In this study, we set out to investigate the positive effect of HDACs on transcription elongation. Our data show that HDAC-regulated transcription elongation requires heat shock protein 90 (HSP90) activity. In contrast, the elongation block that results from CDK9 inhibition does not, suggesting that CDK9 functions downstream of HDACs and HSP90. Treatment with HDACIs causes redistribution of other elongation factors across the genome. Particularly, colocalization of RNAP2 with the NELF complex across the genome, whose stability is regulated by the HSP90 chaperone, is increased strongly after HDACI treatment. These inhibitors induce global acetylation changes, which redistributes BRD4 binding, an important factor involved in promoting enhancer activity, and affects the regulatory organization of the genome. Because BRD4 and NELF are associated with enhancers, we looked at enhancer activity after HDACI treatment. We found that HDACIs reduce eRNA synthesis at high eRNA-producing enhancer sites. This is associated with corresponding changes in the expression of neighboring genes. Overall, we show that HDACs are important regulators of elongation and play an essential role in active gene transcription for many genes.

RESULTS

HDAC Inhibition Blocks Elongation of RNAP2

HDACIs repress transcription by blocking elongation, as we have shown previously in human breast cancer (BT474) and non-cancerous breast epithelial (MCF10A) cell lines using GRO-seq (Kim et al., 2013). Analysis of expression within different gene regions by reads per kilobase of annotated region per million mapped sequence reads (RPKM) normalization indicates that repressed genes have an impediment in the transcription of gene bodies, but the transcription near the start of genes is not changed significantly or is increased after 4-hr treatment with either of two pan-specific HDACIs, TSA and SAHA, in BT474 (Figure 1A; Figure S1A) and MCF10A (Figure 1B; Figure S1A) cells. GRO-seq gene body RPKM was used to classify genes into three groups based on expression changes in response to HDACIs. Genes whose expression goes down after SAHA treatment were defined as repressed, genes whose expression is

unchanged were identified as not changed, and genes whose expression is increased were defined as activated. There is a high percentage of overlap between genes in the three expression change groupings seen in these data compared with GRO-seq data generated previously (Kim et al., 2013) in these cell lines (Table S1). Chromatin immunoprecipitation sequencing (ChIP-seq) of RNAP2 was conducted to validate the three groupings, and we found that SAHA does not significantly change the density of RNAP2 in the promoters of repressed genes (Figure S1B; Table S2). In the gene body, RNAP2 binding decreases in GRO-seq-repressed genes, stays the same in unchanged genes, and increases significantly in activated genes (Figure S1B; Table S3).

To examine the kinetics by which HDACIs suppress transcription elongation, the effect of SAHA treatment for a shorter time was examined in BT474 cells with GRO-seq. SAHA represses genes via an elongation block even after a short 30-min treatment and resulted in a similar, although less intense global pattern of elongation inhibition as the 4-hr treatment (Figures S1C and S1D). To test whether the repressive effect of SAHA on transcription elongation is applicable to cells of a different origin, we applied SAHA to a neuroblastoma cell line, SK-N-SH, and examined the transcription elongation pattern. SAHA blocked elongation in SK-N-SH cells (Figure S1E), underscoring the general applicability of HDACIs as transcription elongation blockers. Overall, our data show that HDAC inhibition blocks the transition of RNAP2 into productive elongation in HDACI-repressed genes in a short time window and in a broad cellular context.

We examined whether overexpression of the HDAC1 isoform can rescue the effect of SAHA to validate that HDACIs are inhibiting the intended target and that HDACIs are causing repression through a block in the catalysis of deacetylation. We overexpressed recombinant HDAC1 wild-type (WT) and catalytically dead mutant (mut; Figure S1F), and examined the expression of two well characterized HDACI-repressed oncogenes regulated by elongation in BT474 cells, *ERBB2* and *MYC* (Kim et al., 2013). Overexpression of the WT HDAC1 isoform, but not mut, in BT474 cells antagonizes SAHA-mediated repression of these two oncogenes (Figure S1G). TSA is also antagonized by HDAC1 overexpression, and the effect of overexpression could be overcome by increasing the dose of the drug (Figure S1H). This demonstrates that HDACIs are repressing transcription by blocking the deacetylation catalyzed by HDAC1, a class I deacetylase, and, possibly, other isoforms. Furthermore, ChIP-seq analysis of HDAC1 shows that, prior to drug treatment, this enzyme is more enriched in genes that can be repressed by SAHA treatment compared with genes that do not change their expression after SAHA (Figure S1I; comparison of DMSO samples). Together, these data suggest that genes that are repressed by HDACI treatment are regulated by deacetylation.

HDACI Repression of Transcription Requires HSP90

The HSP90 chaperone complex promotes RNAP2 pausing in *Drosophila* (Sawarkar et al., 2012). Therefore, we tested whether the mechanism of HDACI suppression of transcription elongation is dependent on HSP90. A potent HSP90 inhibitor, geldanamycin (GEL), was applied to reduce pausing and was used in combination with HDACIs in BT474 cells to see how these small molecules interact to affect elongation. qRT-PCR shows that *ERBB2* and *MYC* repression by HDACIs is antagonized by GEL treatment (Figure 2A), whereas *RPS10* and *ACTG1*, which are not repressed by HDACIs, do not show a significant increase in expression after combination treatment (Figure S2A). To look at the global elongation changes brought on by the drug combinations, we conducted GRO-seq with single and combined treatment with the inhibitors. As expected, treating with GEL alone reduces the amount of promoter-proximal transcripts in both the BT474 and MCF10A cell lines (Figures 2B and 2C; Figure S2B), validating this treatment as a repressor of pausing. GEL antagonizes the repression of the majority of the top 1,000 HDACI-repressed genes (Figures 2D and 2E) more than 5-fold (Figure S2C). Combination treatment with GEL antagonizes the gene body repression induced by HDACIs (Figures 2F and 2G; Figure S3D). These results show that HDACI-mediated repression of elongation is dependent on HSP90 activity.

NELFE, a subunit of the NELF complex, is destabilized upon HSP90 inhibition in cells from several organisms (Sawarkar et al., 2012). Destabilization of just one subunit of the four-subunit NELF complex leads to the degradation of the entire complex (Narita et al., 2007; Sun and Li, 2010; Sun et al., 2008). We tested whether NELF is a downstream effector of HSP90 that could be mediating transcriptional elongation repression by HDACIs. In BT474 cells, GEL destabilizes the NELFA subunit (Figure 3A), which likely leads to the destabilization of the entire NELF complex. To examine the change in binding of NELF upon HDACI treatment, we performed ChIP-seq of NELFA and HSP90 in DMSO- and SAHA-treated BT474 cells. NELFA and HSP90 density are correlated in promoters and gene bodies, with a stronger correlation in gene bodies (Figure 3B). More than half of RNAP2 binding peaks are not colocalized with NELFA in the DMSO treatment control. In contrast, SAHA treatment dramatically increases the number of NELFA peaks, and these peaks predominantly overlap with RNAP2 (Figure 3C). These results show that the global distribution of NELF binding is affected by SAHA, indicating that HDACI treatment may result in transcription pausing through NELF.

P-TEFb Inhibition Affects Transcription Elongation, but Not through HSP90

P-TEFb is an important regulator of elongation, so we sought to determine how P-TEFb might act in connection with HDACs and HSP90. In addition to the HSP90 inhibitor GEL, we used the elongation inhibitor flavopiridol (FLAVO), which inhibits the CDK9 subunit of the P-TEFb complex. We aimed to compare its effects on elongation with HDACI and GEL combination treatment. Like HDACIs, FLAVO represses *ERBB2* and *MYC* transcript levels in BT474 cells (Figure S3A). Globally, FLAVO-repressed genes show a decrease in gene body transcription in GRO-seq experiments. However, unlike HDACI-repressed genes, FLAVO-repressed genes displayed a dramatic increase in promoter-proximal transcription (Figures 4A and 4B; Figure S3B). Furthermore, transcription in the gene bodies of FLAVO-repressed genes in BT474 and MCF10A cells is still repressed in the presence of GEL (Figures 4C and 4D;

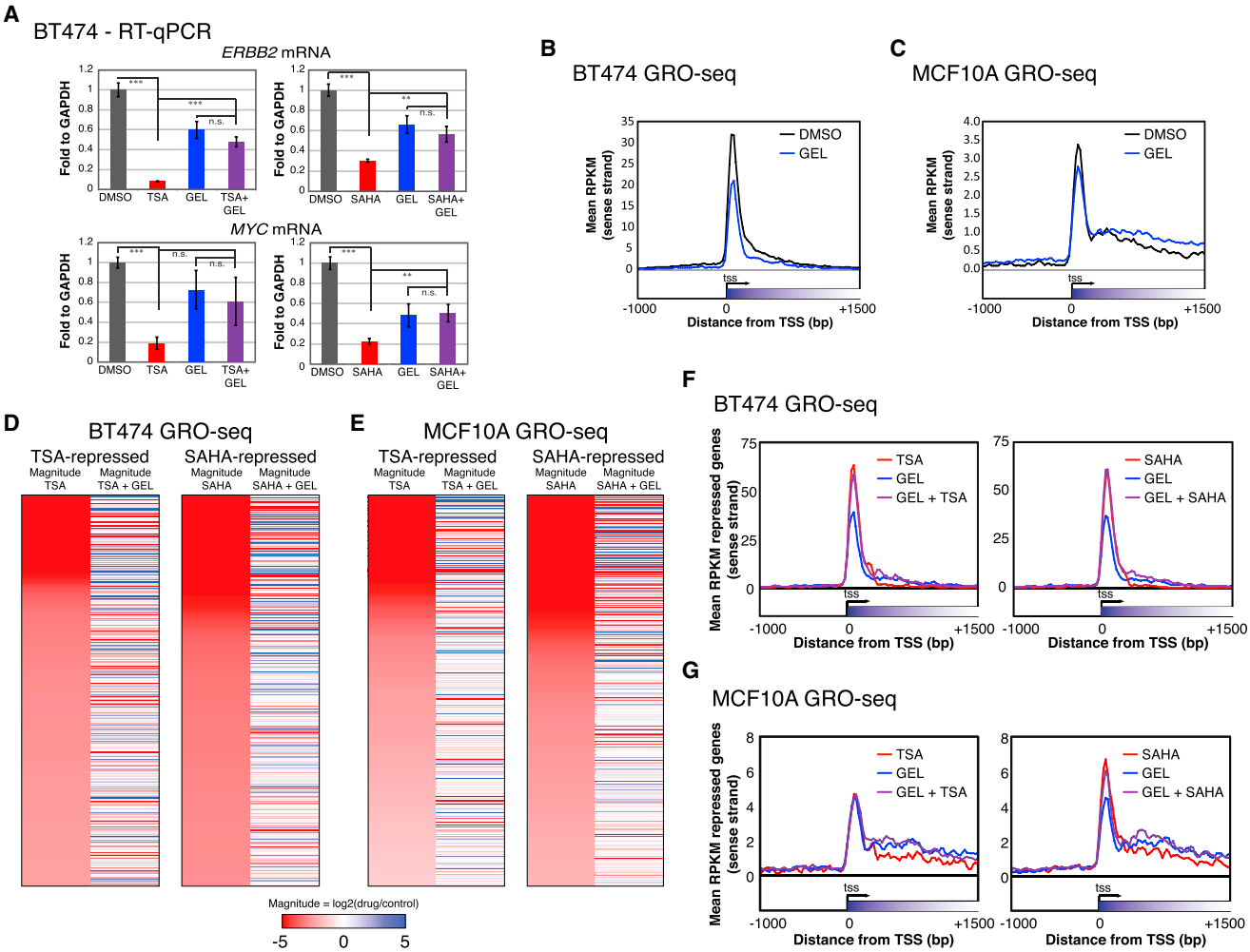

Figure 2. Inhibition of HSP90 Antagonizes HDACI Repression

(A) mRNA level of HDACI-repressed genes in combination with GEL. Quantitation of *ERBB2* and *MYC* mRNA relative to *GAPDH* in BT474 cells after single and combined treatments is shown. Statistical significance was determined with a two-tailed t test. ***$p < 0.001$; **$p < 0.01$; and n.s., not significant ($p > 0.05$). Error bars represent SE. n = 11–14 from at least four biological replicates. GEL was administered at 20 μM.

(B) GRO-seq metagenes of GEL treatment for all genes in BT474 cells. One GRO-seq experiment was conducted. 37,467 genes are represented in the metaplot.

(C) Same as (B) for MCF10A cells.

(D) Heatmaps of the top 1,000 TSA- and SAHA-repressed genes in BT474 cells as determined by GRO-seq and those same genes when GEL was also added. The magnitude of expression for HDACIs was calculated relative to DMSO, and HDACI + GEL was relative to GEL. The colors represent the magnitude expression change in log scale, with red representing repression and blue activation.

(E) Same as (D) for MCF10A cells.

(F) Metagenes of HDACI-repressed genes in BT474 cells when GEL was also added (same genes as in Figure 1A).

(G) Same as (F) for MCF10A cells (same genes as in Figure 1B).

See Figure S2 for qRT-PCR of genes not repressed by HDACIs after combination treatment, GRO-seq statistics, and percentages of genes antagonized by GEL.

Figure S3B), whereas the transcription of HDACI-repressed genes was recovered by GEL treatment (Figures 2D and 2E; Figure S2C). Elongation patterns observed in GRO-seq were examined after combined treatment with these drugs. The FLAVO-induced elongation repression pattern persists in the presence of GEL (Figures 4E and 4F; Figure S3B), suggesting that its mechanism of repression is HSP90-independent. This shows that HDACI-mediated transcription suppression occurs through a different mechanism than FLAVO. Perhaps FLAVO suppresses elongation via more immediate effects on the phosphorylation of RNAP2 CTD than HDACIs, which suppress genes under tight control of HSP90.

Acetylation and BRD4 Binding Changes in Gene Bodies and Intergenically after HDACI

HDACI treatment globally increases acetylation, and we predicted that this results in changes in the distribution of the binding of key acetylated histone readers such as BRD4. This protein acts as a scaffold to recruit elongation factors, so its redistribution would lead to changes in the binding of other proteins.

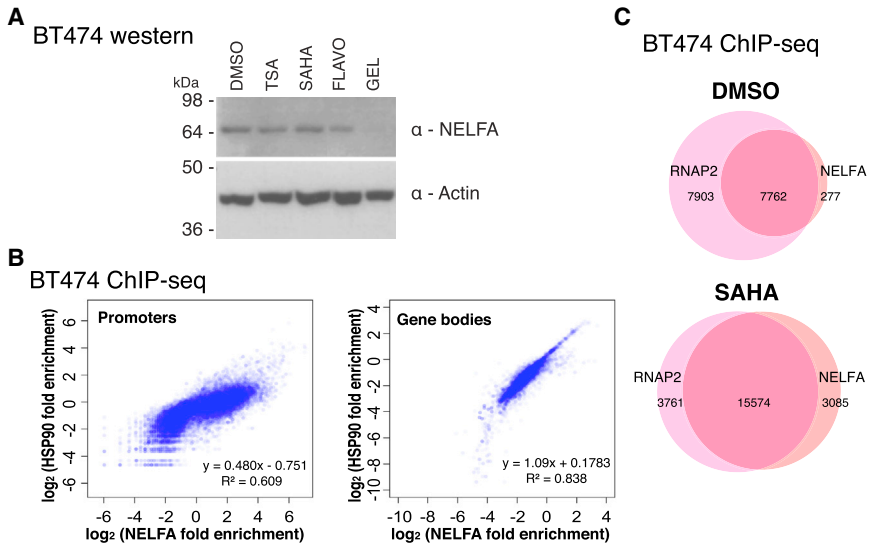

Figure 3. HSP90 Stabilizes NELFA, and SAHA Increases NELFA Binding

(A) NELFA stability after treatment with different elongation-affecting drugs, shown with western blot of BT474 cell lysates (representative image for one of two blots).

(B) Correlation of NELFA and HSP90 fold enrichments in promoter and gene body regions for 33,119 annotated RefSeq genes. Two biological replicates for each ChIP-seq were conducted, and the average signal is plotted.

(C) Venn diagrams of RNAP2 and NELFA peak overlaps. Overlaps were within a 500-bp window. The numbers of genes in each section are shown.

ChIP-seq shows that the acetylation of lysines in histone H3K27 (H3K27Ac), H3 (H3Ac), and H4 (H4Ac) is reduced in promoter-proximal regions, whereas, in gene bodies, acetylation increases after SAHA treatment (Figure 5A). Consistent with the changes in acetylation, SAHA treatment decreases the binding of BRD4 near TSSs and increases its binding in gene bodies (Figure 5B; Tables S2 and S3). BRD4 is enriched in repressed genes more than in unchanged genes in BT474 cells without inhibitor treatment, suggesting that their transcription is regulated by BRD4 under normal conditions, unlike the unchanged genes.

Interestingly, we noticed that, in gene coding regions, although the magnitude of BRD4 binding and acetylation may differ, the locations of detected peaks did not show many changes upon SAHA treatment (Figure 6A). In intergenic regions, however, there are much more striking changes in the location of peaks, and there is an increase in the number of peaks by SAHA treatment (Figure 6B), suggesting that HDACIs may affect the global chromatin landscape far beyond regions encoding genes.

To investigate whether changes in BRD4 binding are correlated with changes in acetylation, we identified whether peaks were maintained after SAHA treatment. We identified sites where BRD4 binding peaks were lost (only present in DMSO), overlap (present in both DMSO and SAHA), and gained (only present after SAHA treatment). We determined the magnitude of change in the acetylation and binding at these sites. As expected, BRD4 binding is reduced at sites where BRD4 is lost, stays the same at overlapping sites, and increases at gained sites (Figure 6C). At these same sites, the level of acetylation is similar at lost and overlap sites but displays far greater increases at gained sites (Figure 6D). Therefore, BRD4 is being recruited to newly created sites of acetylation in intergenic regions. Loss of BRD4 binding at certain sites after SAHA treatment may be due to newly created acetylated sites competing for the binding of this protein.

JQ1, a BRD4 inhibitor, and HDACIs share similar gene expression change profiles (Bhadury et al., 2014). To see which genes were mutually affected by BRD4, HDAC, or P-TEFb inhibition, we defined the top 1,000 most repressed genes for each drug and determined the percentage of genes the inhibitors were able to repress in pairwise combinations. The percentage of genes shared between JQ1 and the HDACIs is similar to the percentage shared between the two related HDACIs, TSA and SAHA. FLAVO does not have as large of an overlap with HDACIs as JQ1, indicating more similarity between the effects of BRD4 and HDAC inhibition than P-TEFb inhibition (Figure S4A). Concordantly, JQ1 represses *ERBB2* and *MYC* in BT474 cells (Figure S4B). This drug also represses elongation in a pattern similar to HDACIs in our two cell lines (Figures S4C and S4D). This indicates that JQ1 and HDACIs may have a similar mechanism of action.

eRNA Transcription Is Repressed by HDACIs

BRD4 is bound at active enhancers (Chapuy et al., 2013), and it has been found recently that JQ1 reduces eRNA synthesis (Kanno et al., 2014). Because restructuring of acetylation and BRD4 binding occurs in intergenic regions, we wondered whether HDACI treatment could be affecting positive regulators of transcription located in intergenic regions, namely enhancers, via loss of BRD4 at pertinent enhancer sites. We used a prediction method similar to the one defined by the Ozato group (Kanno et al., 2014) to find eRNA-generating sites by determining intergenic BRD4 peak locations in BT474 cells from ChIP-seq and characterized the level of eRNA synthesis around them (Figure 7A). As validation, we showed that the enrichment of H3K27Ac, a mark of active enhancers, is higher at predicted enhancer sites than at annotated promoters (Figure 7B). The expression of the most highly expressed eRNAs from a 4-hr DMSO treatment were analyzed in comparison with their expression after different inhibitor treatments (Figure 7C). JQ1, as expected from previous reports, reduced eRNAs. HDACIs did as well, and to an even greater extent. Even after only 30 min of SAHA treatment, the inhibitor was able to reduce eRNAs (Figure S5A), showing that this treatment causes fast action at enhancers. Both BRD4 and HDACs are therefore positive regulators of enhancer activity, possibly through effects of HDACIs on BRD4 binding (Figure 6; Figure S5B). In contrast, FLAVO did not decrease the median eRNA synthesis level at enhancers, suggesting that eRNA transcription is P-TEFb-independent. Surprisingly, GEL treatment is a strong repressor of eRNA

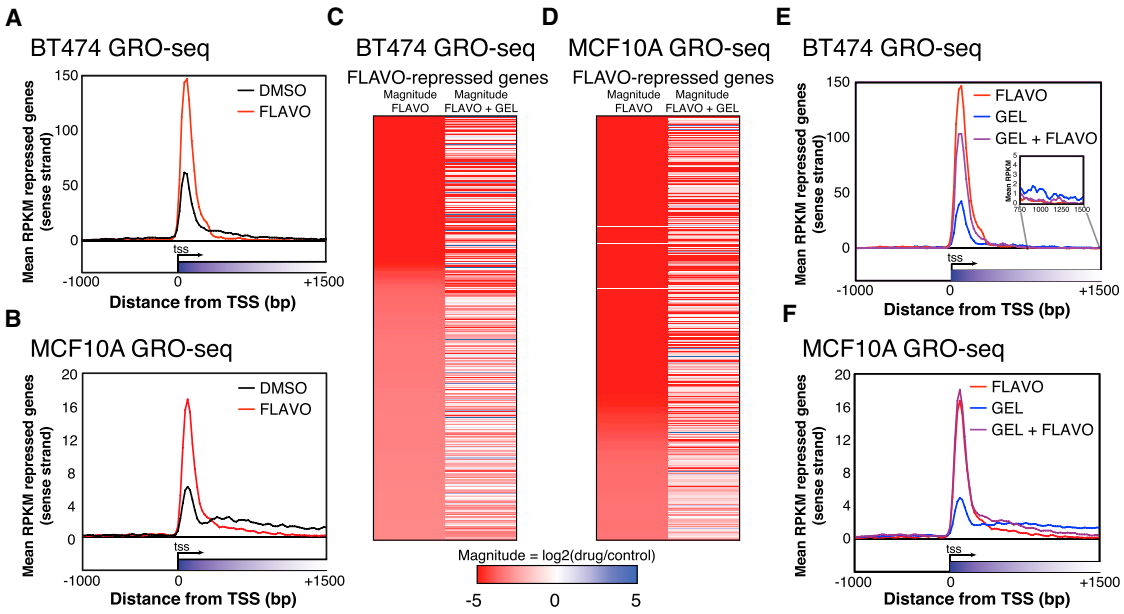

Figure 4. Elongation Block Caused by P-TEFb Inhibition Is Not Dependent on HSP90

(A) FLAVO-repressed (log-likelihood ratio $p < 10^{-20}$ for gene body RPKM changes, 9,706 genes) metagenes from BT474 cells. Data are from one GRO-seq experiment.

(B) Same as (A) for MCF10A cells (12,659 genes).

(C) Heatmaps of the expression changes in the top 1,000 FLAVO-repressed genes with the greatest magnitude of change in BT474 cells, as determined by GRO-seq (log-likelihood ratio $p < 10^{-20}$), and those same genes when GEL was also added. The colors indicate the magnitude expression change in log scale. Red represents repression and blue activation.

(D) Same as (C) for MCF10A cells.

(E) Metagenes of all FLAVO-repressed genes when GEL was also added to BT474 cells.

(F) Same as (E) for MCF10A cells.

See also Figure S3 for FLAVO repression of *ERBB2* and *MYC* and GRO-seq statistics.

synthesis, indicating that HSP90 is necessary for enhancer function and, possibly, linking NELF to enhancer function because of the effect HSP90 has on NELF stability. As in the BT474 cell line, HDACI treatment reduces eRNAs in MCF10A cells, as do JQ1 and GEL. FLAVO, again, does not repress eRNAs (Figure S5C), demonstrating that the effect of HDACI on enhancers is not cancer-specific. We tested whether these enhancers are regulating genes nearby because, although enhancers can work from a great distance, they often regulate nearby genes. We looked at the percentage of genes near eRNA sites that are reduced significantly by inhibitor treatment. We found that, compared with the percentage of all genes that are repressed by an inhibitor, there is a higher percentage of genes repressed that are located near downregulated eRNA sites (Figure 7D; Figure S5D). This suggests that the eRNA activity level affects target gene expression and shows that enhancer activity is dependent on HDACs.

DISCUSSION

The repression of transcription by HDACIs in many genes is counterintuitive because of the well-known role HDACs play in turning off transcription. We have shown that HDACIs cause a block in the elongation step of transcription by RNAP2. Some studies show evidence to support this finding. First, HDACs bind to highly expressed genes more than to lowly expressed genes and heterochromatin, suggesting that they play a role in active gene transcription (Wang et al., 2009). This is in line with our previous finding that HDACIs target the most highly expressed genes for repression (Kim et al., 2013). Second, single-cell imaging experiments show that, shortly after induction of transcription initiation, acetylation of histones is decreased around the time that the elongating form of RNAP2 is detected (Stasevich et al., 2014). The deacetylation caused by classical HDACs post-initiation is likely an important step in inducing gene body transcription and may suggest that cycling of acetylation and deacetylation is important in the process of transcription elongation (Wang et al., 2009).

Based on our analysis, HDACs are required for the removal of acetylation marks in gene bodies and intergenic regions, where their levels are lower than at promoters and enhancers. We know that, in yeast, the RPD3 deacetylase, related to class I HDACs in humans, acts to specifically deacetylate gene bodies. It is recruited by the histone H3 lysine 36 methylation (H3K36me) mark, which is deposited cotranscriptionally along with the elongating RNAP2 (Carrozza et al., 2005; Joshi and Struhl, 2005). When the cell is unable to deacetylate these sites because of the presence of HDACIs, the acetylation enriched near promoters and enhancers may no longer serve to demarcate these regulatory regions from the rest of the genome. BRD4, which is lost at promoters and redistributed

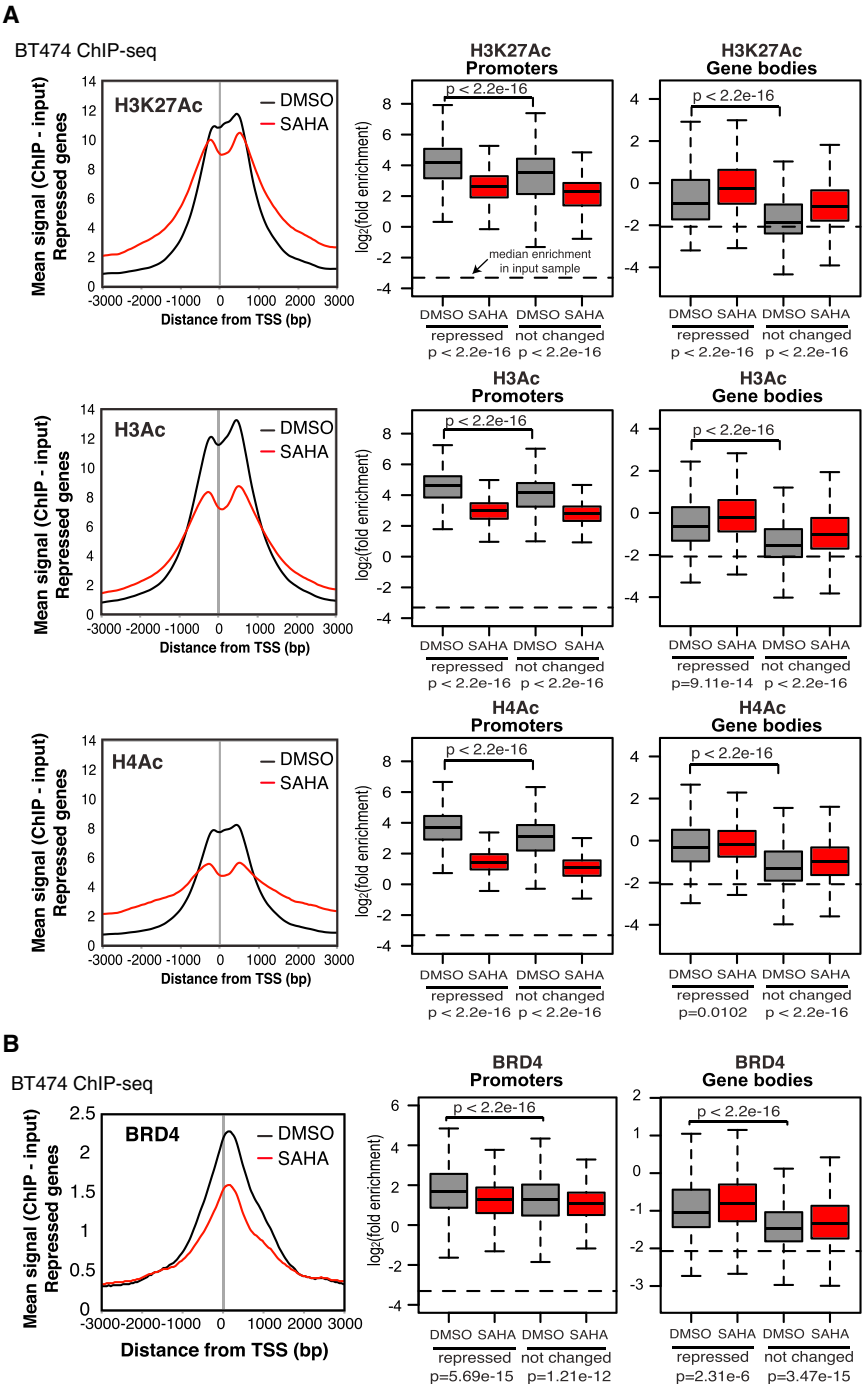

Figure 5. HDACIs Affect Acetylation of Histones and BRD4 Binding

(A) ChIP-seq profiles of acetylated histone tails around TSSs of repressed genes and their enrichment in promoters and gene bodies. Average acetyl-ChIP-seq profiles from two biological replicates are averaged and normalized to the average yield of both replicates. The H3Ac antibody recognizes acetylated K9 and K14 in the H3 subunit. The H4Ac antibody recognizes acetylated K5, K8, K12, and K16 in the H4 subunit.

(B) BRD4 binding at TSSs and in gene bodies of repressed genes. Quantitation of their binding in repressed and unchanged genes is shown in boxplots. The statistics reported are from Wilcoxon rank-sum tests. Horizontal lines on the boxplot graphs represent the median signal in all genes from the chromatin input sample. Shown is the average of two replicates.

intergenically after HDACI treatment, is important in the recruitment of elongation factors to appropriate locations to activate transcription. Indeed, HDACs are required for BRD4-inducible transcription in human cell lines (Hu et al., 2014). The reduction in BRD4 likely leads to the reduction of the factors it recruits, such as P-TEFb, at promoters after HDACI treatment. Other elongation factors may also redistribute in response to BRD4 binding to inappropriate acetylation marks when HDACs are not able to maintain a lower level of acetylation at specific sites. More work is required to determine whether BRD4 binding partners are responsible for the block in elongation after applying HDACIs or whether BRD4 redistribution itself exerts this effect on elongation.

HDACIs appear to work upstream of P-TEFb and require HSP90 activity. HDAC inhibition affects NELF binding, and HDACIs cannot repress transcription in the presence of GEL. This may be through the stabilization of the NELF complex as well as effects on other client proteins of HSP90 involved in elongation (Schaaf et al., 2013; Zhou et al., 2015). Although there are multiple known acetylation sites on HSP90, all seem to reduce the interaction of HSP90 with client proteins (Kovacs et al., 2005; Scroggins et al., 2007; Yang et al., 2008), opposite of what would be expected based on the results reported here. HDACIs have also been shown to change the levels of reactive oxygen species in the cell, which induces some HSP90 degradation (Park et al., 2015), but this, again, contradicts the increase in NELF binding after HDACI treatment. So it may be that HDACIs regulate elongation by directly affecting NELF or other elongation factors and that these factors require HSP90 to stabilize them. Whether there are intermediate steps between HDAC function and NELF activity is unknown.

Here we report that eRNA production is reduced when HDACs are inhibited. They are also reduced when HSP90, which is responsible for NELF stability, is repressed. This may further explain how HDACIs repress transcription because enhancer function and elongation are possibly linked via NELF function

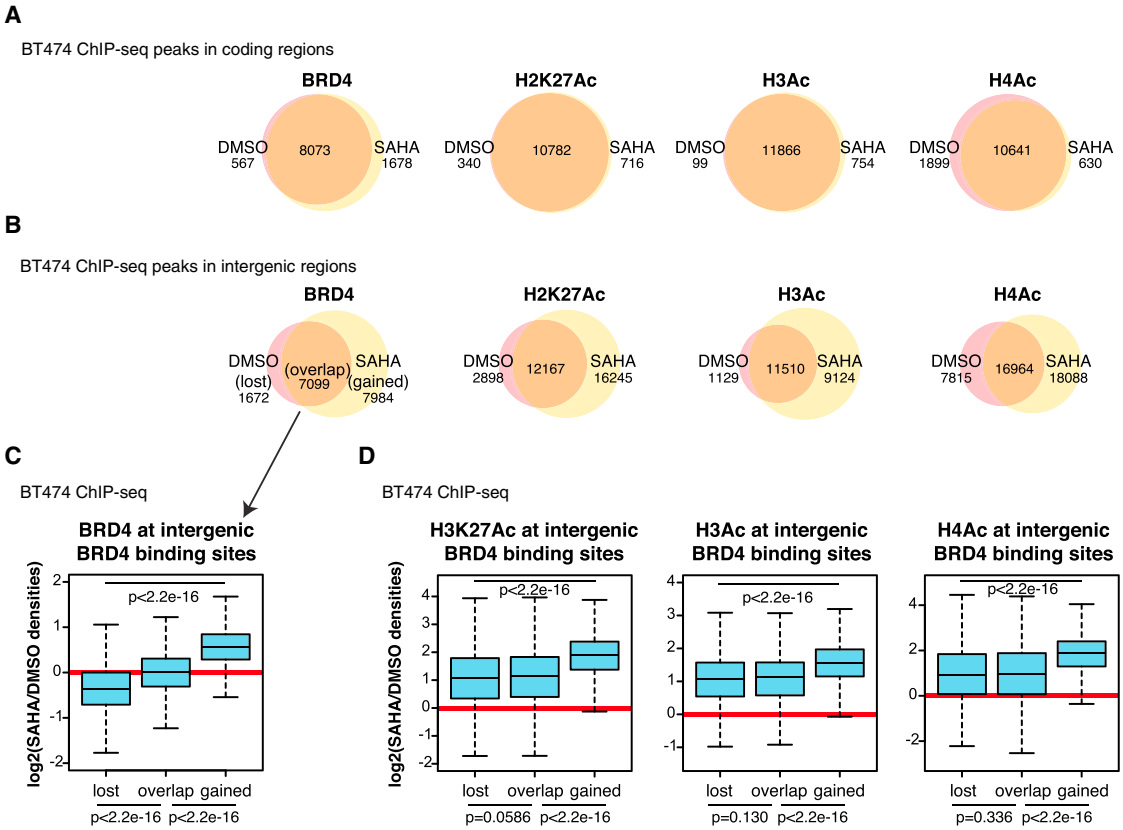

Figure 6. Intergenic Changes in BRD4 Binding and Corollary Changes in Histone Acetylation

(A) Peaks and their overlaps before and after SAHA treatment in coding regions for acetylated histones and BRD4 in BT474 cells.

(B) Peaks and their overlaps before and after SAHA treatment in intergenic regions for acetylated histones and BRD4 in BT474 cells. The number of peaks in each category is listed. Only peaks present in both replicates were considered.

(C) Within intergenic BRD4 binding sites, those that are lost upon SAHA, stay bound, and are gained after SAHA are analyzed for intensity of BRD4 binding changes.

(D) Acetylation changes at intergenic BRD4 binding sites.

See also Figure S4 for the overlap of genes affected by TSA, SAHA, JQ1 (BRD4 inhibitor), and FLAVO treatments and JQ1 effects on *ERBB2* and *MYC* expression and elongation.

(Schaukowitch et al., 2014). Further analysis of which genes these enhancers regulate is required to fully understand the effects HDACs and NELF have on enhancer activity.

Going forward, it will be important to identify relevant targets of acetylation that are necessary for transcriptional activation by HDACs in histones or other proteins because deacetylation of non-histone substrates may also be involved in promoting transcription elongation. A large amount of lysine acetylation events on non-histone substrates have been identified globally using mass spectrometry, and BRD4, several HDAC isoforms, SPT5 (a DSIF component), and NELFB all have acetylated lysines (Choudhary et al., 2009) that could have effects on elongation. Functional analysis of these sites will help determine how they affect this pathway. Also, biochemical analysis of elongation factors after HSP90 inhibition would be beneficial to elucidate how this factor affects their stability and function.

HDACIs are an effective treatment for several types of cancer (Federico and Bagella, 2011). These drugs globally increase acetylation, which is often associated with an increase in the transcription level of many genes, and they increase the expression of many important cell cycle arrest and apoptotic genes (Xu et al., 2007). In contrast, we have also found that many oncogenes are selectively targeted for repression by HDACIs through effects on elongation because of their high level of transcription (Kim et al., 2013). The elongation pathway may be a very useful therapeutic target for cancer because other elongation-inhibiting drugs, like FLAVO and JQ1, have also shown promise as cancer treatments (Filippakopoulos et al., 2010; Patel et al., 1998; Zuber et al., 2011). Understanding the mechanism by which HDACIs strengthen elongation blocks may facilitate the development of treatments able to more specifically target genes for therapeutic repression.

EXPERIMENTAL PROCEDURES

Cell Culture

MCF10A, BT474, and SK-N-SH cells were obtained from the American Type Culture Collection (ATCC) and cultured according to their suggested conditions.

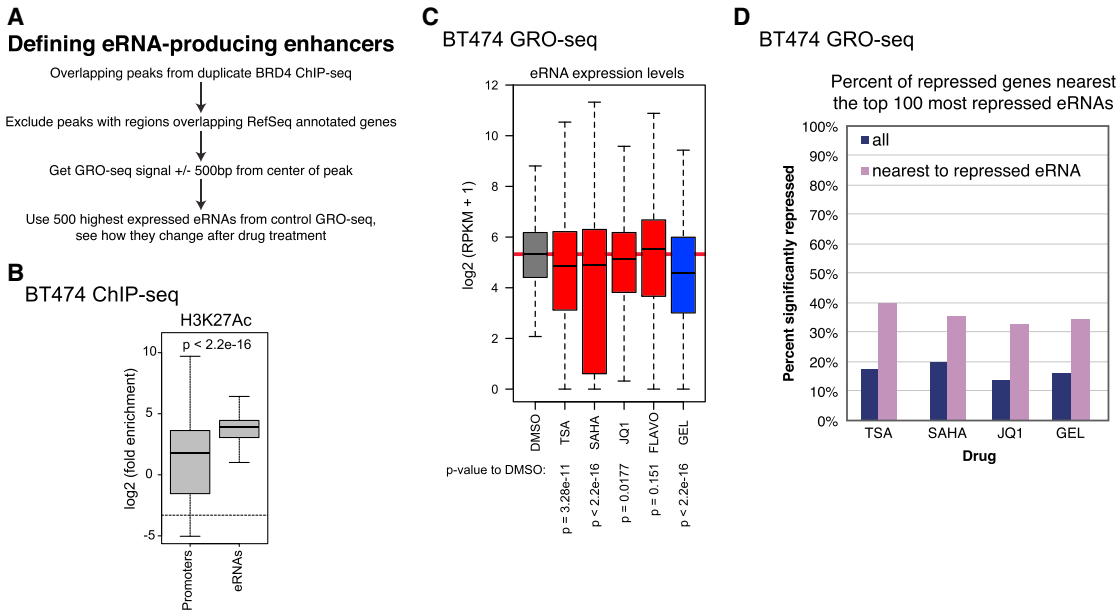

Figure 7. eRNA Expression Is Reduced by HDACIs

(A) BRD4 intergenic binding sites were defined, and GRO-seq reads were aligned to a 1,000-bp window around the center of the peak. The top 500 most expressed eRNAs were identified in a DMSO GRO-seq experiment and analyzed in DMSO and under different drug conditions.

(B) Enrichment of H3K27Ac at predicted enhancer sites compared with annotated promoters.

(C) Boxplot of eRNA expression after different drug treatments. Statistics are from Wilcoxon rank-sum tests.

(D) Percentage of genes that are repressed either overall or only in the genes closest to the top 100 most repressed eRNAs for each drug.

See also Figure S5 for eRNA expression changes after a 30-min SAHA treatment, the binding changes of BRD4 at predicted enhancer sites, and the changes in eRNA production brought on by inhibitor treatments in MCF10A cells.

Drug Treatments

TSA and SAHA were obtained from Sigma (SAHA lot no. 042M4740V), (S)-JQ1 was a gift from J. Bradner at the Dana Farber Cancer Institute (DFCI), FLAVO was from Sigma (lot no. 100M4723V), and GEL was from Enzo Life Sciences (BML-EI280).

For GRO-seq, the doses were 500 nM, 5 μM, 500 nM, 500 nM, and 10 μM for TSA, SAHA, JQ1, FLAVO, and GEL, respectively. 4-hr treatments were done for the elongation inhibitors TSA, SAHA, JQ1, and FLAVO, and GEL was applied for 4 hr and 15 min (15-min pre-treatment of GEL for combined GEL plus elongation inhibitor treatments). The 30-min SAHA treatment for GRO-seq was the exception. 4-hr treatments were used for DMSO, SAHA, and FLAVO ChIP-seq experiments and 24-hr treatments for qRT-PCR and western blot samples unless stated otherwise.

Expression Analysis

qRT-PCR was performed as described previously (Kim et al., 2013) except with the ImProm-II enzyme from Promega with 4.6875 mM $MgCl_2$ in the reverse-transcriptase reaction. The *MYC* primer sequences are *MYC*-F 5′-CTCTGACCTTTTGCCAGGAG-3′ and *MYC*-R 5′-TCCTCGGATTCTCTGC TCTC-3′.

Western Blot

Western blots were done with the same NELFA antibody as that used in ChIP-seq or polyclonal rabbit V5 antibody from Abcam (catalog no. ab9116). BT474 cells were treated for 24 hr before lysis.

GRO-Seq

GRO-seq was performed as described previously (Kim et al., 2013), except the detergent concentration was optimized and libraries were multiplexed to conduct high-throughput sequencing in one lane. Additional details can be found in the Supplemental Experimental Procedures.

ChIP

Chromatin was prepared and immunoprecipitated as described previously (Kim et al., 2011), except that protein A/G dynabeads (Invitrogen) were used instead of organism-specific secondary antibody bound beads. 25% of the amount of chromatin was used for RNAP2 and acetyl ChIPs to reduce oversaturation of bead binding. Details regarding antibodies used can be found in the Supplemental Experimental Procedures.

ChIP-Seq Library Preparation

The ThruPLEX DNA-seq kit from Rubicon Genomics was used for multiplexed ChIP-seq library prep of BT474 chromatin. Indexed samples were quantitated with qPCR and mixed in equimolar amounts. The input sample was prepared with an Illumina DNA-seq kit.

Sequencing and Sequencing Data Analysis

The Yale Stem Cell Center Genomics and Bioinformatics Core Facility conducted the sequencing on an Illumina HiSeq 2000 platform. Sequencing data alignment and normalization are described in the Supplemental Experimental Procedures.

Metagenes of GRO-seq data were generated with scripts from H. Kwak (Kwak et al., 2013) and are shown as 25-base pair (bp) windows considering transcript directionality. ChIP-seq metagenes were generated with our own perl scripts, which count ChIP-seq and input reads and normalize read counts by the total number of mapped reads in 50-bp sliding windows. Directionality of the gene was not considered. Boxplots and Venn diagrams were created using R version 3.1.2.

Peaks were called with MACS 1.3.7.1 (Zhang et al., 2008) with the mfold parameter set to 10. BEDTools v2.23.0 (Glass and Rosenfeld, 2000) was used to generate overlaps between duplicate samples and identify peaks and signals coming from genic and intergenic regions, and the multicov

function was used to determine the amount of signal coming from a given genomic region.

In BT474 cells, eRNA annotation was done by taking peaks called in model-based analysis for ChIP-seq (MACS) for BRD4, removing regions within 1 kilobase of Refseq-annotated genes. BEDTools was used to find overlapping peaks between replicates. Partek was used to find the amount of reads coming from 500 bp upstream and downstream of the center of the BRD4 peaks. The highest expressed putative eRNAs in a DMSO treatment from an independently generated GRO-seq experiment was used to sort the highest expressed eRNAs, and then the DMSO from the same experiment as the other treated samples acted as the control. Genes nearest to the predicted eRNA sites were determined using BEDTools closest function.

Statistical Tests and Categorizations

Two-tailed Student's t tests and R^2 were performed in Excel 14.4.9. Wilcoxon rank-sum tests were performed in R version 3.1.2, and the p values reported are not corrected for multiple testing. Statistical analysis for defining repression or activation in GRO-seq was performed using the log-likelihood ratio in the Partek Genomic Suite, version 6.14.0220.

GRO-seq expression level change groupings for ChIP-seq were determined by selecting significantly repressed or activated genes (log-likelihood ratio, $p < 10^{-20}$) based on gene body RPKM in DMSO and SAHA treatments. Unchanged genes were expressed in DMSO and SAHA conditions, were not changed significantly ($p > 10^{-20}$), and had less than a 2-fold change in their expression, up or down. The genes common to these categorized lists from the GRO-seq prepared for this manuscript and the GRO-seq prepared previously (Kim et al., 2013) were used to analyze ChIP-seq data (Table S1).

Additional methods and associated references are available in the Supplemental Information.

ACCESSION NUMBERS

The accession numbers for the GRO-seq and ChIP-seq data reported in this paper are ArrayExpress: E-MTAB-3626, E-MTAB-3631

SUPPLEMENTAL INFORMATION

Supplemental Information includes Supplemental Experimental Procedures, five figures, and three tables and can be found with this article online at http://dx.doi.org/10.1016/j.celrep.2015.10.013.

AUTHOR CONTRIBUTIONS

C.B.G. designed, performed, and analyzed experiments; made the figures; wrote scripts; interpreted data; and wrote the manuscript. T.H.K. conceived the project, provided overall direction, and secured funding for the project. Y.T. wrote scripts for the analysis of ChIP-seq data. Y.J.K. worked with Y.T. to develop the data analysis and oversaw sequencing library preparation. P.X. and M.Q.Z. contributed to the annotation of putative eRNA sites in MCF10A. I.H.P. and T.H.K. discussed the results and edited the manuscript.

ACKNOWLEDGMENTS

We are grateful to James Bradner (Harvard Medical School) for providing us with JQ1. We thank Y. Zhang and G. Greer for technical help with cloning. C.B.G. has received support from NIH Training Grant GM007324 and a PhRMA foundation predoctoral fellowship. MQZ and PX acknowledge support from NIH Grant R01 MH102616, the Cecil H. and Ida Green Endowment Chair, and a UTD Founder's Fellowship. I.H.P. is partly supported by NIGMS (GM0099130-01, GM111667-01), the KRIBB/KRCF research initiative program (NAP-09-1), and a CT Stem Cell Grant (13-SCB-YALE-06). Grants to T.H.K. from the Rita Allen Foundation, Sidney Kimmel Foundation for Cancer Research, Yale Comprehensive Cancer Center (CA-16359), Alexander and Margaret Stewart Trust, National Institute of Allergy and Infection Disease (R21AI107067), and National Cancer Institute (R01CA140485) supported this work.

Received: June 22, 2015
Revised: August 26, 2015
Accepted: October 6, 2015
Published: November 5, 2015

REFERENCES

Adelman, K., and Lis, J.T. (2012). Promoter-proximal pausing of RNA polymerase II: emerging roles in metazoans. Nat. Rev. Genet. *13*, 720–731.

Banerjee, A.R., Kim, Y.J., and Kim, T.H. (2014). A novel virus-inducible enhancer of the interferon-β gene with tightly linked promoter and enhancer activities. Nucleic Acids Res. *42*, 12537–12554.

Bhadury, J., Nilsson, L.M., Muralidharan, S.V., Green, L.C., Li, Z., Gesner, E.M., Hansen, H.C., Keller, U.B., McLure, K.G., and Nilsson, J.A. (2014). BET and HDAC inhibitors induce similar genes and biological effects and synergize to kill in Myc-induced murine lymphoma. Proc. Natl. Acad. Sci. USA *111*, E2721–E2730.

Bolden, J.E., Peart, M.J., and Johnstone, R.W. (2006). Anticancer activities of histone deacetylase inhibitors. Nat. Rev. Drug Discov. *5*, 769–784.

Carrozza, M.J., Li, B., Florens, L., Suganuma, T., Swanson, S.K., Lee, K.K., Shia, W.J., Anderson, S., Yates, J., Washburn, M.P., and Workman, J.L. (2005). Histone H3 methylation by Set2 directs deacetylation of coding regions by Rpd3S to suppress spurious intragenic transcription. Cell *123*, 581–592.

Chapuy, B., McKeown, M.R., Lin, C.Y., Monti, S., Roemer, M.G., Qi, J., Rahl, P.B., Sun, H.H., Yeda, K.T., Doench, J.G., et al. (2013). Discovery and characterization of super-enhancer-associated dependencies in diffuse large B cell lymphoma. Cancer Cell *24*, 777–790.

Chen, H., Lin, R.J., Xie, W., Wilpitz, D., and Evans, R.M. (1999). Regulation of hormone-induced histone hyperacetylation and gene activation via acetylation of an acetylase. Cell *98*, 675–686.

Chou, C.W., Wu, M.S., Huang, W.C., and Chen, C.C. (2011). HDAC inhibition decreases the expression of EGFR in colorectal cancer cells. PLoS ONE *6*, e18087.

Choudhary, C., Kumar, C., Gnad, F., Nielsen, M.L., Rehman, M., Walther, T.C., Olsen, J.V., and Mann, M. (2009). Lysine acetylation targets protein complexes and co-regulates major cellular functions. Science *325*, 834–840.

Core, L.J., Waterfall, J.J., and Lis, J.T. (2008). Nascent RNA sequencing reveals widespread pausing and divergent initiation at human promoters. Science *322*, 1845–1848.

Danko, C.G., Hyland, S.L., Core, L.J., Martins, A.L., Waters, C.T., Lee, H.W., Cheung, V.G., Kraus, W.L., Lis, J.T., and Siepel, A. (2015). Identification of active transcriptional regulatory elements from GRO-seq data. Nat. Methods *12*, 433–438.

Delmore, J.E., Issa, G.C., Lemieux, M.E., Rahl, P.B., Shi, J., Jacobs, H.M., Kastritis, E., Gilpatrick, T., Paranal, R.M., Qi, J., et al. (2011). BET bromodomain inhibition as a therapeutic strategy to target c-Myc. Cell *146*, 904–917.

Eberharter, A., and Becker, P.B. (2002). Histone acetylation: a switch between repressive and permissive chromatin. Second in review series on chromatin dynamics. EMBO Rep. *3*, 224–229.

Federico, M., and Bagella, L. (2011). Histone deacetylase inhibitors in the treatment of hematological malignancies and solid tumors. J. Biomed. Biotechnol. *2011*, 475641.

Filippakopoulos, P., Qi, J., Picaud, S., Shen, Y., Smith, W.B., Fedorov, O., Morse, E.M., Keates, T., Hickman, T.T., Felletar, I., et al. (2010). Selective inhibition of BET bromodomains. Nature *468*, 1067–1073.

Fujinaga, K., Irwin, D., Huang, Y., Taube, R., Kurosu, T., and Peterlin, B.M. (2004). Dynamics of human immunodeficiency virus transcription: P-TEFb phosphorylates RD and dissociates negative effectors from the transactivation response element. Mol. Cell. Biol. *24*, 787–795.

Gilchrist, D.A., Dos Santos, G., Fargo, D.C., Xie, B., Gao, Y., Li, L., and Adelman, K. (2010). Pausing of RNA polymerase II disrupts DNA-specified nucleosome organization to enable precise gene regulation. Cell *143*, 540–551.

Glass, C.K., and Rosenfeld, M.G. (2000). The coregulator exchange in transcriptional functions of nuclear receptors. Genes Dev. *14*, 121–141.

Hsieh, C.L., Fei, T., Chen, Y., Li, T., Gao, Y., Wang, X., Sun, T., Sweeney, C.J., Lee, G.S., Chen, S., et al. (2014). Enhancer RNAs participate in androgen receptor-driven looping that selectively enhances gene activation. Proc. Natl. Acad. Sci. USA *111*, 7319–7324.

Hu, X., Lu, X., Liu, R., Ai, N., Cao, Z., Li, Y., Liu, J., Yu, B., Liu, K., Wang, H., et al. (2014). Histone cross-talk connects protein phosphatase 1α (PP1α) and histone deacetylase (HDAC) pathways to regulate the functional transition of bromodomain-containing 4 (BRD4) for inducible gene expression. J. Biol. Chem. *289*, 23154–23167.

Jang, M.K., Mochizuki, K., Zhou, M., Jeong, H.S., Brady, J.N., and Ozato, K. (2005). The bromodomain protein Brd4 is a positive regulatory component of P-TEFb and stimulates RNA polymerase II-dependent transcription. Mol. Cell *19*, 523–534.

Jin, F., Li, Y., Dixon, J.R., Selvaraj, S., Ye, Z., Lee, A.Y., Yen, C.A., Schmitt, A.D., Espinoza, C.A., and Ren, B. (2013). A high-resolution map of the three-dimensional chromatin interactome in human cells. Nature *503*, 290–294.

Joshi, A.A., and Struhl, K. (2005). Eaf3 chromodomain interaction with methylated H3-K36 links histone deacetylation to Pol II elongation. Mol. Cell *20*, 971–978.

Kanno, T., Kanno, Y., LeRoy, G., Campos, E., Sun, H.W., Brooks, S.R., Vahedi, G., Heightman, T.D., Garcia, B.A., Reinberg, D., et al. (2014). BRD4 assists elongation of both coding and enhancer RNAs by interacting with acetylated histones. Nat. Struct. Mol. Biol. *21*, 1047–1057.

Kim, Y.J., Cecchini, K.R., and Kim, T.H. (2011). Conserved, developmentally regulated mechanism couples chromosomal looping and heterochromatin barrier activity at the homeobox gene A locus. Proc. Natl. Acad. Sci. USA *108*, 7391–7396.

Kim, Y.J., Greer, C.B., Cecchini, K.R., Harris, L.N., Tuck, D.P., and Kim, T.H. (2013). HDAC inhibitors induce transcriptional repression of high copy number genes in breast cancer through elongation blockade. Oncogene *32*, 2828–2835.

Kovacs, J.J., Murphy, P.J., Gaillard, S., Zhao, X., Wu, J.T., Nicchitta, C.V., Yoshida, M., Toft, D.O., Pratt, W.B., and Yao, T.P. (2005). HDAC6 regulates Hsp90 acetylation and chaperone-dependent activation of glucocorticoid receptor. Mol. Cell *18*, 601–607.

Kwak, H., and Lis, J.T. (2013). Control of transcriptional elongation. Annu. Rev. Genet. *47*, 483–508.

Kwak, H., Fuda, N.J., Core, L.J., and Lis, J.T. (2013). Precise maps of RNA polymerase reveal how promoters direct initiation and pausing. Science *339*, 950–953.

Lovén, J., Hoke, H.A., Lin, C.Y., Lau, A., Orlando, D.A., Vakoc, C.R., Bradner, J.E., Lee, T.I., and Young, R.A. (2013). Selective inhibition of tumor oncogenes by disruption of super-enhancers. Cell *153*, 320–334.

Melo, C.A., Drost, J., Wijchers, P.J., van de Werken, H., de Wit, E., Oude Vrielink, J.A., Elkon, R., Melo, S.A., Léveillé, N., Kalluri, R., et al. (2013). eRNAs are required for p53-dependent enhancer activity and gene transcription. Mol. Cell *49*, 524–535.

Moreau, P., Hen, R., Wasylyk, B., Everett, R., Gaub, M.P., and Chambon, P. (1981). The SV40 72 base repair repeat has a striking effect on gene expression both in SV40 and other chimeric recombinants. Nucleic Acids Res. *9*, 6047–6068.

Narita, T., Yung, T.M., Yamamoto, J., Tsuboi, Y., Tanabe, H., Tanaka, K., Yamaguchi, Y., and Handa, H. (2007). NELF interacts with CBC and participates in 3′ end processing of replication-dependent histone mRNAs. Mol. Cell *26*, 349–365.

Park, S., Park, J.A., Kim, Y.E., Song, S., Kwon, H.J., and Lee, Y. (2015). Suberoylanilide hydroxamic acid induces ROS-mediated cleavage of HSP90 in leukemia cells. Cell Stress Chaperones *20*, 149–157.

Patel, V., Senderowicz, A.M., Pinto, D., Jr., Igishi, T., Raffeld, M., Quintanilla-Martinez, L., Ensley, J.F., Sausville, E.A., and Gutkind, J.S. (1998). Flavopiridol, a novel cyclin-dependent kinase inhibitor, suppresses the growth of head and neck squamous cell carcinomas by inducing apoptosis. J. Clin. Invest. *102*, 1674–1681.

Sawarkar, R., Sievers, C., and Paro, R. (2012). Hsp90 globally targets paused RNA polymerase to regulate gene expression in response to environmental stimuli. Cell *149*, 807–818.

Schaaf, C.A., Kwak, H., Koenig, A., Misulovin, Z., Gohara, D.W., Watson, A., Zhou, Y., Lis, J.T., and Dorsett, D. (2013). Genome-wide control of RNA polymerase II activity by cohesin. PLoS Genet. *9*, e1003382.

Schaukowitch, K., Joo, J.Y., Liu, X., Watts, J.K., Martinez, C., and Kim, T.K. (2014). Enhancer RNA facilitates NELF release from immediate early genes. Mol. Cell *56*, 29–42.

Scott, G.K., Marden, C., Xu, F., Kirk, L., and Benz, C.C. (2002). Transcriptional repression of ErbB2 by histone deacetylase inhibitors detected by a genomically integrated ErbB2 promoter-reporting cell screen. Mol. Cancer Ther. *1*, 385–392.

Scroggins, B.T., Robzyk, K., Wang, D., Marcu, M.G., Tsutsumi, S., Beebe, K., Cotter, R.J., Felts, S., Toft, D., Karnitz, L., et al. (2007). An acetylation site in the middle domain of Hsp90 regulates chaperone function. Mol. Cell *25*, 151–159.

Shlyueva, D., Stampfel, G., and Stark, A. (2014). Transcriptional enhancers: from properties to genome-wide predictions. Nat. Rev. Genet. *15*, 272–286.

Stasevich, T.J., Hayashi-Takanaka, Y., Sato, Y., Maehara, K., Ohkawa, Y., Sakata-Sogawa, K., Tokunaga, M., Nagase, T., Nozaki, N., McNally, J.G., and Kimura, H. (2014). Regulation of RNA polymerase II activation by histone acetylation in single living cells. Nature *516*, 272–275.

Sterner, D.E., and Berger, S.L. (2000). Acetylation of histones and transcription-related factors. Microbiol. Mol. Biol. Rev. *64*, 435–459.

Sun, J., and Li, R. (2010). Human negative elongation factor activates transcription and regulates alternative transcription initiation. J. Biol. Chem. *285*, 6443–6452.

Sun, J., Watkins, G., Blair, A.L., Moskaluk, C., Ghosh, S., Jiang, W.G., and Li, R. (2008). Deregulation of cofactor of BRCA1 expression in breast cancer cells. J. Cell. Biochem. *103*, 1798–1807.

Thomas, M.C., and Chiang, C.M. (2006). The general transcription machinery and general cofactors. Crit. Rev. Biochem. Mol. Biol. *41*, 105–178.

Vidal, M., and Gaber, R.F. (1991). RPD3 encodes a second factor required to achieve maximum positive and negative transcriptional states in Saccharomyces cerevisiae. Mol. Cell. Biol. *11*, 6317–6327.

Vidal, M., Strich, R., Esposito, R.E., and Gaber, R.F. (1991). RPD1 (SIN3/UME4) is required for maximal activation and repression of diverse yeast genes. Mol. Cell. Biol. *11*, 6306–6316.

Wang, A., Kurdistani, S.K., and Grunstein, M. (2002). Requirement of Hos2 histone deacetylase for gene activity in yeast. Science *298*, 1412–1414.

Wang, Z., Zang, C., Cui, K., Schones, D.E., Barski, A., Peng, W., and Zhao, K. (2009). Genome-wide mapping of HATs and HDACs reveals distinct functions in active and inactive genes. Cell *138*, 1019–1031.

Wolf, D., Rodova, M., Miska, E.A., Calvet, J.P., and Kouzarides, T. (2002). Acetylation of beta-catenin by CREB-binding protein (CBP). J. Biol. Chem. *277*, 25562–25567.

Wu, C.H., Yamaguchi, Y., Benjamin, L.R., Horvat-Gordon, M., Washinsky, J., Enerly, E., Larsson, J., Lambertsson, A., Handa, H., and Gilmour, D. (2003). NELF and DSIF cause promoter proximal pausing on the hsp70 promoter in Drosophila. Genes Dev. *17*, 1402–1414.

Xu, M., Nie, L., Kim, S.H., and Sun, X.H. (2003). STAT5-induced Id-1 transcription involves recruitment of HDAC1 and deacetylation of C/EBPbeta. EMBO J. *22*, 893–904.

Xu, W.S., Parmigiani, R.B., and Marks, P.A. (2007). Histone deacetylase inhibitors: molecular mechanisms of action. Oncogene *26*, 5541–5552.

Yamaguchi, Y., Takagi, T., Wada, T., Yano, K., Furuya, A., Sugimoto, S., Hasegawa, J., and Handa, H. (1999). NELF, a multisubunit complex containing RD, cooperates with DSIF to repress RNA polymerase II elongation. Cell *97*, 41–51.

Yamaguchi, Y., Inukai, N., Narita, T., Wada, T., and Handa, H. (2002). Evidence that negative elongation factor represses transcription elongation through

binding to a DRB sensitivity-inducing factor/RNA polymerase II complex and RNA. Mol. Cell. Biol. *22*, 2918–2927.

Yang, Z., Yik, J.H., Chen, R., He, N., Jang, M.K., Ozato, K., and Zhou, Q. (2005). Recruitment of P-TEFb for stimulation of transcriptional elongation by the bromodomain protein Brd4. Mol. Cell *19*, 535–545.

Yang, Y., Rao, R., Shen, J., Tang, Y., Fiskus, W., Nechtman, J., Atadja, P., and Bhalla, K. (2008). Role of acetylation and extracellular location of heat shock protein 90alpha in tumor cell invasion. Cancer Res. *68*, 4833–4842.

Zhai, S., Senderowicz, A.M., Sausville, E.A., and Figg, W.D. (2002). Flavopiridol, a novel cyclin-dependent kinase inhibitor, in clinical development. Ann. Pharmacother. *36*, 905–911.

Zhang, Y., Liu, T., Meyer, C.A., Eeckhoute, J., Johnson, D.S., Bernstein, B.E., Nusbaum, C., Myers, R.M., Brown, M., Li, W., and Liu, X.S. (2008). Model-based analysis of ChIP-Seq (MACS). Genome Biol. *9*, R137.

Zhou, X., Fan, L.X., Peters, D.J., Trudel, M., Bradner, J.E., and Li, X. (2015). Therapeutic targeting of BET bromodomain protein, Brd4, delays cyst growth in ADPKD. Hum. Mol. Genet. *24*, 3982–3993.

Zuber, J., Shi, J., Wang, E., Rappaport, A.R., Herrmann, H., Sison, E.A., Magoon, D., Qi, J., Blatt, K., Wunderlich, M., et al. (2011). RNAi screen identifies Brd4 as a therapeutic target in acute myeloid leukaemia. Nature *478*, 524–528.